DONNAN POTENTIAL AND SURFACE POTENTIAL OF A CHARGED MEMBRANE

HIROYUKI OHSHIMA AND SHINPEI OHKI
Department of Biophysical Sciences, State University of New York at Buffalo, Buffalo, New York 14214

ABSTRACT A model is presented for the electrical potential distribution across a charged biological membrane that is in equilibrium with an electrolyte solution. We assume that a membrane has charged surface layers of thickness d on both surfaces of the membrane, where the fixed charges are distributed at a uniform density N within the layers, and that these charged layers are permeable to electrolyte ions. This model unites two different concepts, that is, the Donnan potential and the surface potential (or the Gouy-Chapman double-layer potential). Namely, the present model leads to the Donnan potential when $d \gg 1/\kappa'$ (κ' is the Debye-Hückel parameter of the surface charge layer) and to the surface potential as $d \to 0$, keeping the product Nd constant. The potential distribution depends significantly on the thickness d of the surface charge layer when $d \lesssim 1/\kappa'$.

INTRODUCTION

When a biological membrane, which usually has net negative fixed charges, is in equilibrium with an electrolyte solution, electric potential difference is generally established between the membrane and the solution. There have been two entirely different approaches to this potential difference (Davies and Rideal, 1961). One approach considers the potential difference to be the Donnan equilibrium potential. This approach has particularly been used for studies of ion transport processes through membrane (Teorell, 1953). In the other approach it is regarded as the surface potential, i.e., the Gouy-Chapman double-layer potential, which is familiar in colloid sciences (Verwey and Overbeek, 1948).

When a membrane that is permeable to electrolyte ions and contains negatively charged groups at a uniform density N, is in equilibrium with a symmetrical electrolyte solution of concentration n and valence Z, the Donnan potential ψ_D relative to the external bulk solution is expressed as (Davies and Rideal, 1961; Ohki, 1965).

$$\psi_D = -\frac{kT}{Ze}\ln\left\{\frac{N}{2Zn}+\left[\left(\frac{N}{2Zn}\right)^2+1\right]^{1/2}\right\} = -\frac{kT}{Ze}\operatorname{arc\,sinh}\left(\frac{N}{2Zn}\right), \quad (1)$$

where k is the Boltzmann constant, T the absolute temperature, and e the elementary electric charge. Conventionally, the Donnan potential is considered to be accompanied by a discontinuous potential gap across the membrane surface (Fig. 1 *a*). This is due to the assumption of local electroneutrality, which is used in the classical derivation of Eq. 1. To be exact, however, as Mauro (1962) has done, this assumption must be replaced by the Poisson equation (or the Poisson-Boltzmann equation if the Boltzmann distribution can be assumed for electrolyte ions). Mauro (1962) showed that this replacement leads to a continuous Donnan potential that diffuses over distances of order $1/\kappa$ (κ is the Debye-Hückel parameter) on both sides of the membrane surface as shown in Fig. 1 *b* (in this diffuse region, local electroneutrality no longer holds).

If, on the other hand, it is assumed that all the membrane fixed charges are located only at the membrane surface and the electrolyte ions cannot penetrate into the membrane, then the electrical double layer is considered to be formed around the surface (Fig. 1 *c*) and the surface potential relative to the bulk solution takes the following form (Verwey and Overbeek, 1948; Davies and Rideal, 1961), which is quite different from Eq. 1

$$\psi_s = \frac{2kT}{Ze}\operatorname{arc\,sinh}\left[\frac{\sigma}{(8n\epsilon_r\epsilon_0 kT)^{1/2}}\right], \quad (2)$$

where σ is the surface charge density of the membrane, ϵ_r the relative permittivity of the solution, and ϵ_0 the permittivity of a vacuum. Several modifications on the surface potential approach have been attempted by allowing the surface region to be permeable to electrolyte ions in relation to cell-cell interactions (Parsegian and Gingell, 1973; Parsegian, 1974) and to cell electrophoresis (Haydon, 1961; Donath and Pastushenko, 1979; Wunderlich, 1982; Levine et al., 1983).

In spite of the above-mentioned improvements or modifications on each of the two different approaches, there still remains ambiguity as to the inter-relation or transition

Address all correspondence to Dr. S. Ohki.

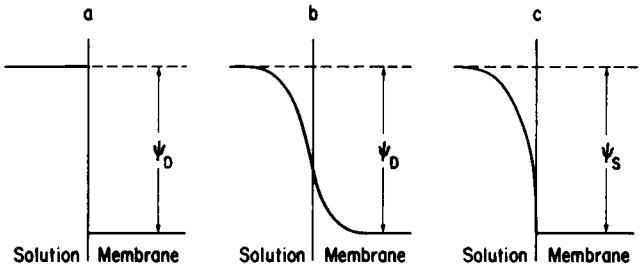

FIGURE 1 Schematic representation of the potential distribution near the membrane surface by the hitherto proposed models: (*a*) classical (discontinuous) Donnan potential; (*b*) continuous Donnan potential (Mauro, 1962); (*c*) surface potential.

between the Donnan potential and the surface potential. We present here a model for the potential distribution across a charged membrane, in which the membrane fixed charges are uniformly distributed through a layer of finite thickness (which is permeable to electrolyte ions) at the membrane surface. We solve exactly the nonlinear Poisson-Boltzmann equation for the outside and inside regions of the membrane and show that this model smoothly connects the Donnan and surface potential concepts.

MODEL

We suppose a planar charged membrane that is in equilibrium with a large volume of a symmetrical electrolyte solution of concentration n and valence Z. We choose the x-axis in the direction normal to the membrane surface so that the plane at $x = 0$ coincides with the left boundary between the membrane and the solution (Fig. 2). We consider the membrane to be composed of three layers: two identical surface layers of thickness d, which contain negatively charged groups at a uniform density N and are permeable to electrolyte ions ($0 \leqq x \leqq d$ and $h + d \leqq x \leqq h + 2d$), and one core layer of thickness h, which has no fixed charges and is impermeable to ions ($d \leqq x \leqq h + d$). Since the membrane considered here is symmetrical with respect to the plane $x = h/2 + d$, we need to consider only the region $-\infty < x \leqq h/2 + d$.

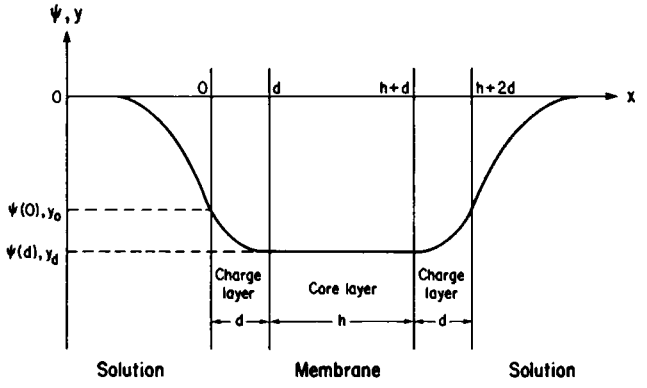

FIGURE 2 Schematic representation of the potential distribution $\psi(x)$ across a membrane with two surface charge layers (of thickness d) and one core layer (of thickness h).

We assume that the electrical potential $\psi(x)$ at position x in the regions $x < 0$ and $0 < x < d$ (relative to the bulk solution [$x = -\infty$]) satisfies the Poisson-Boltzmann equation (in SI units)

$$\frac{d^2\psi}{dx^2} = \frac{2Zen}{\epsilon_r\epsilon_0}\sinh\frac{Ze\psi}{kT}, \quad x < 0, \tag{3}$$

$$\frac{d^2\psi}{dx^2} = \frac{2Zen}{\epsilon_r'\epsilon_0}\sinh\frac{Ze\psi}{kT} + \frac{eN}{\epsilon_r'\epsilon_0}, \quad 0 < x < d, \tag{4}$$

where ϵ_r and ϵ_r' are the relative permittivities of the solution and of the surface charge layer, respectively. For the region $d < x \leqq h/2 + d$, in which there are no true charges, we have

$$\frac{d^2\psi}{dx^2} = 0, \quad d < x < h/2 + d. \tag{5}$$

The boundary conditions are

$$\psi(x) \text{ is continuous at } x = 0 \text{ and } x = d, \text{ and} \tag{6}$$

$$\epsilon_r\left.\frac{d\psi}{dx}\right|_{-0} = \epsilon_r'\left.\frac{d\psi}{dx}\right|_{+0} \tag{7}$$

$$\epsilon_r'\left.\frac{d\psi}{dx}\right|_{d-0} = \epsilon_r''\left.\frac{d\psi}{dx}\right|_{d+0}, \tag{8}$$

$$\psi(x) \xrightarrow[x\to-\infty]{} 0, \tag{9}$$

where ϵ_r'' is the relative permittivity of the core layer; and because of symmetry of the membrane, we have

$$\left.\frac{d\psi}{dx}\right|_{h/2+d} = 0. \tag{10}$$

Integrating Eq. 5 and using Eq. 10, we have

$$\frac{d\psi}{dx} = 0, \quad d < x \leqq h/2 + d, \tag{11}$$

which can also be obtained directly from the fact that due to symmetry there is no electric field within the core layer. It follows from Eq. 11 that the right-hand side of Eq. 8 becomes zero, and thus the boundary condition (Eq. 8) may be replaced by

$$\left.\frac{d\psi}{dx}\right|_{d-0} = 0. \tag{12}$$

The solution of Eqs. 3 and 4 subject to the boundary conditions Eqs. 6, 7, 9, and 12 completely determines the potential function $\psi(x)$ in our system. We now introduce the following dimensionless potential

$$y = \frac{Ze\psi}{kT}. \tag{13}$$

Then, Eqs. 3 and 4 are reduced to

$$\frac{d^2y}{dx^2} = \kappa^2 \sinh y, \qquad x < 0 \tag{14}$$

$$\frac{d^2y}{dx^2} = \kappa'^2\left(\sinh y + \frac{N}{2Zn}\right), \qquad 0 < x < d \tag{15}$$

and the boundary conditions of Eqs. 6, 7, 9, and 12 are reduced to the following:

$$y \text{ is continuous at } x = 0 \text{ and } x = d, \text{ and} \tag{16}$$

$$\epsilon_r \frac{dy}{dx}\bigg|_{-0} = \epsilon_r' \frac{dy}{dx}\bigg|_{+0} \tag{17}$$

$$y \xrightarrow[x \to -\infty]{} 0, \tag{18}$$

$$\frac{dy}{dx}\bigg|_{-0} = 0, \tag{19}$$

where

$$\kappa = \left(\frac{2nZ^2e^2}{\epsilon_r\epsilon_0 kT}\right)^{1/2} \tag{20}$$

and

$$\kappa' = \left(\frac{2nZ^2e^2}{\epsilon_r'\epsilon_0 kT}\right)^{1/2} \tag{21}$$

are, respectively, the Debye-Hückel parameters of the solution and of the surface charged layer, which are related to each other by

$$\frac{\kappa'}{\kappa} = \left(\frac{\epsilon_r}{\epsilon_r'}\right)^{1/2} \tag{22}$$

Eq. 14 subject to the boundary condition of Eq. 18 can easily be integrated to give

$$y = 4 \operatorname{arc\,tanh}\left[\tanh\frac{y_0}{4} e^{-\kappa|x|}\right], \qquad x < 0, \tag{23}$$

from which we obtain

$$\frac{dy}{dx}\bigg|_{-0} = 2\kappa \sinh\frac{y_0}{2}, \tag{24}$$

where we have defined y_0 as

$$y_0 = y(0) = \frac{Ze}{kT}\psi(0). \tag{25}$$

Integration of Eq. 15 subject to the boundary condition of Eq. 19 yields

$$\frac{dy}{dx} = -\kappa'\left[2(\cosh y - \cosh y_d) + \frac{N}{Zn}(y - y_d)\right]^{1/2}, \qquad 0 < x < d \tag{26}$$

where y_d is defined by

$$y_d = y(d) = \frac{Ze}{kT}\psi(d). \tag{27}$$

Evaluating Eq. 26 at $x \to 0$ and using Eq. 16, we obtain

$$\frac{dy}{dx}\bigg|_{+0} = -\kappa'\left[2(\cosh y_0 - \cosh y_d) + \frac{N}{Zn}(y_0 - y_d)\right]^{1/2}. \tag{28}$$

Substituting Eqs. 24 and 28 into Eq. 17 and using Eq. 22, we obtain

$$2\sinh\frac{y_0}{2} = -\left(\frac{\epsilon_r'}{\epsilon_r}\right)^{1/2}\left[2(\cosh y_0 - \cosh y_d) + \frac{N}{Zn}(y_0 - y_d)\right]^{1/2}. \tag{29}$$

Eq. 26 can further be integrated to give

$$\kappa' x = \int_y^{y_0} \frac{dy}{\left[2(\cosh y - \cosh y_d) + \frac{N}{Zn}(y - y_d)\right]^{1/2}}, \qquad 0 < x < d \tag{30}$$

which determines y as an implicit function of x. Eq. 30 becomes as $x \to d$

$$\kappa' d = \int_{y_d}^{y_0} \frac{dy}{\left[2(\cosh y - \cosh y_d) + \frac{N}{Zn}(y - y_d)\right]^{1/2}}. \tag{31}$$

Eqs. 29 and 31 form coupled transcendental and integral equations for y_0 and y_d. By use of obtained values for y_0 and y_d, the potential y at an arbitrary point x can be calculated from Eqs. 23 and 30. For the special case of $\kappa' d = \infty$, to which Eq. 31 is inapplicable, instead of treating Eqs. 30 and 31 we directly solve the differential Eq. 26 numerically to obtain $y(x)$ for $0 < x < \infty$.

Limiting Cases of $d \to \infty$ and $d \to 0$

Case of $d \to \infty$. We treat first the limiting case of $d \to \infty$, that is, the case in which the membrane itself is a semi-infinite charge layer. Mauro (1962) considered this problem for $\epsilon_r = \epsilon_r'$. When $d \to \infty$, the region $0 < x < d$ where Eq. 15 is applicable is extended to the region $0 < x < +\infty$, so that

$$\frac{d^2y}{dx^2} = \kappa'^2\left(\sinh y + \frac{N}{2Zn}\right), \qquad 0 < x < +\infty \tag{32}$$

and the total potential difference across the membrane $\psi(d)$ (or y_d) becomes equal to $\psi(+\infty)$ (or $y[\infty]$). Noting

that $d^2y/dx^2 = 0$ at $x = +\infty$, from Eq. 32 we obtain

$$y_\infty = y(\infty) = -\operatorname{arc\,sinh}\frac{N}{2Zn}, \tag{33}$$

which agrees with the Donnan potential (Eq. 1). We note that Eq. 33 does not depend on ϵ_r or ϵ_r'.

Figs. 3 and 4 illustrate two examples of numerical calculations of the potential distribution across the membrane surface with $d = \infty$ when $T = 298°K$, $Z = 1$, $n = 0.1$ M, $\epsilon_r = 78.5$, $\epsilon_r'/\epsilon_r = 1$ and 0.5, $N = 0.686$ M (Fig. 3) and $N = 10.7$ M (Fig. 4), the values of N being chosen so as to give $\psi(\infty) = -50$ and -120 mV, respectively. As these figures show, $\psi(x)$ (or $y[x]$) diffuses over some distances on both sides of the plane $x = 0$. For $x < 0$, $y(x)$ is given by Eq. 23, showing the Gouy-Chapman type diffuse layer with the decay distance of order $1/\kappa$.

To see how $y(x)$ $(x > 0)$ approaches to y_∞, that is, the behavior of $y(x)$ near y_∞, we put $y = y_\infty + \Delta y$ $(\Delta y \ll 1)$ in Eq. 32 and linearize with respect to Δy. Noting that $\sinh(y + \Delta y) \approx \sinh y_\infty + \cosh y_\infty \cdot \Delta y$ for $\Delta y \ll 1$ and using Eq. 33, we have

$$\frac{d^2\Delta y}{dx^2} = \kappa'^2\left[1 + \left(\frac{N}{2Zn}\right)^2\right]^{1/2}\Delta y, \qquad 0 < x < +\infty. \tag{34}$$

From the solution Δy $(= y - y_\infty)$ of Eq. 34 satisfying the boundary conditions that $y \to y_\infty$ (or $\Delta y \to 0$) as $x \to \infty$ and $y \to y_0$ (or $\Delta y \to y_0 - y_\infty$) as $x \to 0$, we finally obtain for y

$$y = y_\infty + (y_0 - y_\infty)\exp\left[-\kappa'\left\{1 + \left(\frac{N}{2Zn}\right)^2\right\}^{1/4}x\right], \qquad 0 < x < +\infty, \tag{35}$$

which agrees with Mauro's result (1962) when $\epsilon_r'/\epsilon_r = 1$, $Z = 1$, and $N/2n \gg 1$. It follows from Eq. 35 that the thickness of the diffuse layer formed inside the membrane

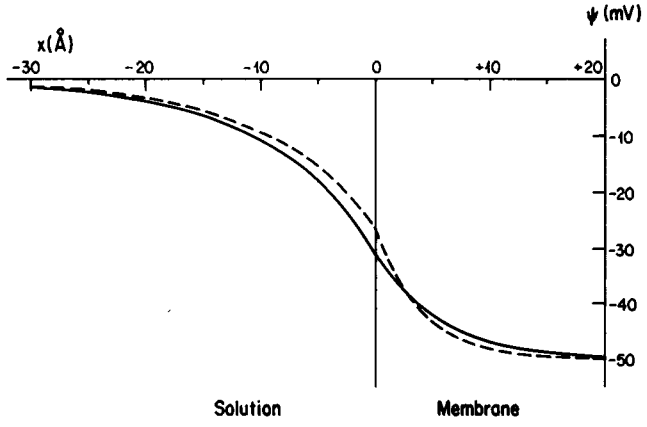

FIGURE 3 Potential distribution $\psi(x)$ across the charged membrane with $d = \infty$. Calculated with $T = 298°K$, $Z = 1$, $n = 0.686$ M, $\epsilon_r'/\epsilon_r = 1$ (solid line), and $\epsilon_r'/\epsilon_r = 0.5$ (broken line).

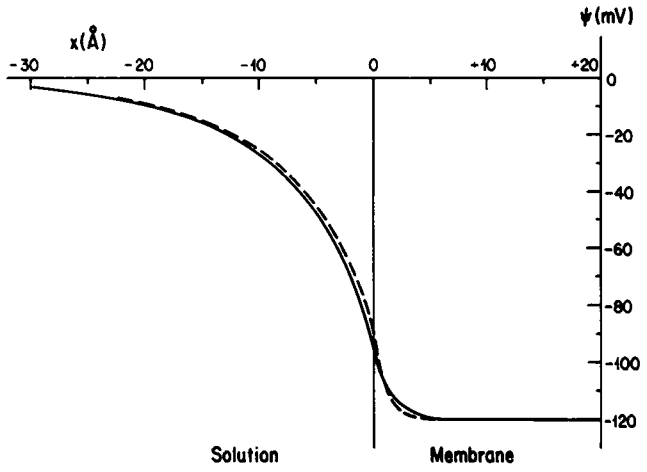

FIGURE 4 The same as in Fig. 3 except for $N = 10.7$ M.

is of the order of $1/\kappa_m$, κ_m being defined as

$$\kappa_m = \kappa'\left[1 + \left(\frac{N}{2Zn}\right)^2\right]^{1/4} \tag{36}$$

and that $y(x)$ approaches to y_∞ more rapidly with increasing ratio $N/2n$ and with decreasing ϵ_r', as is indeed seen in Figs. 3 and 4 (in Fig. 3, $1/\kappa_m \approx 5.1$ Å for $\epsilon_r'/\epsilon_r = 1$ and 3.6 Å for $\epsilon_r'/\epsilon_r = 0.5$; and in Fig. 4, $1/\kappa_m \approx 1.3$ Å for $\epsilon_r'/\epsilon_r = 1$ and 0.9 Å for $\epsilon_r'/\epsilon_r = 0.5$). This can be explained as follows. The concentration of cations just outside the membrane is very large. For these concentrated cations, the membrane negative fixed charges play a role of counter ions and exert the shielding effect. Therefore as N increases, this shielding effect becomes large, reducing the diffuse layer thickness $1/\kappa_m$. The effect of ϵ_r' reflects the polarization of the membrane; the degree of this polarization decreases with decreasing ϵ_r', leading to a larger potential drop inside the membrane.

From the fact that $\psi(x)$ decays over distances of order $1/\kappa_m$ inside the membrane, it follows that if the charge layer thickness d is finite but much $> 1/\kappa_m$ (i.e., $\kappa_m d \gg 1$), the potential distribution across the membrane surface is practically identical to that for a semi-infinite charge layer.

Case of $d \to 0$. Consider next the limiting case of $d \to 0$. Noting that $y - y_d \ll 1$ $(0 < x < d)$ when $\kappa' d \ll 1$, we put $y = y_d + \Delta y$ $(\Delta y \ll 1)$ in the integrand of Eq. 31 and linearize it with respect to Δy by using the same method as used to derive Eq. 34. Then we find

$$\kappa' d = 2\left[\frac{y_0 - y_d}{2\sinh y_d + N/(Zn)}\right]^{1/2}, \qquad \kappa' d \ll 1. \tag{37}$$

Similarly we obtain from Eq. 29

$$2\sinh\frac{y_0}{2} = -\left[\left(\frac{\epsilon_r'}{\epsilon_r}\right)\left(2\sinh y_d + \frac{N}{Zn}\right)(y_0 - y_d)\right]^{1/2}. \tag{38}$$

Eliminating $y_0 - y_d$ from Eqs. 37 and 38, and using Eqs. 20 and 22, we find

$$2\sinh\frac{y_0}{2} = -\frac{eNd}{(2n\epsilon_r\epsilon_0 kT)^{1/2}} - \kappa d\sinh y_d. \tag{39}$$

If we take the limit $d \to 0$ in Eq. 39, keeping the product Nd constant, i.e., keeping the total amount of membrane fixed charges $-eNd$ contained in a unit area of the surface charge layer ($0 < x < d$) constant, then the second term on the right-hand side of Eq. 39 becomes negligible and we obtain the following limiting result, which is identical to Eq. 2

$$y_0 = y_d = 2\,\text{arc sinh}\left[\frac{\sigma}{(8n\epsilon_r\epsilon_0 kT)^{1/2}}\right], \tag{40}$$

where we have defined σ as

$$\sigma = -e\lim_{\substack{d\to 0\\ Nd=\text{constant}}}(Nd), \tag{41}$$

which can be interpreted as the surface charge density of the membrane.

Transition between the Donnan and Surface Potentials

In the preceding section we have shown that our model leads to the continuous Donnan potential when $\kappa_m d \gg 1$ (this condition may be replaced by the condition $\kappa' d \gg 1$, since $\kappa_m > \kappa'$) and to the surface potential as $d \to 0$. To see the transition between these two limiting cases, we consider here the potential distribution for $\kappa' d \lesssim 1$. To perform numerical calculations of $y(x)$ ($0 < x < d$) in the range of $\kappa' d \lesssim 1$, it is most convenient to use the Taylor expansion series of $y(x)$.

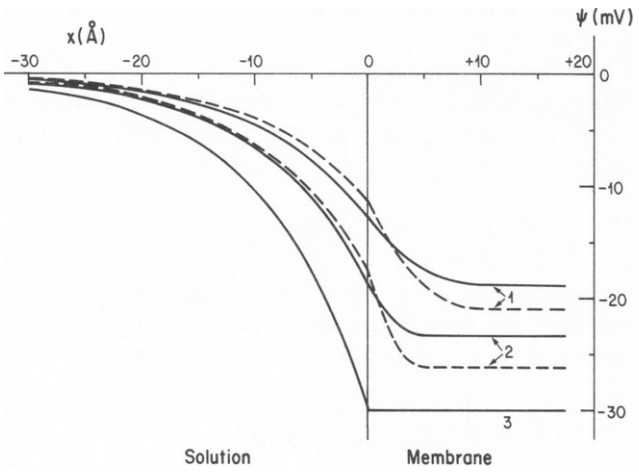

FIGURE 5 Potential distribution $\psi(x)$ across the charged membrane with d = 10, 5, and 0 Å (curves 1, 2, and 3, respectively). Calculated with T = 298°K, Z = 1, n = 0.1 M, $-eND = -0.0229$ C · m^{-2}, ϵ_r'/ϵ_r = 1 (solid lines), and ϵ_r'/ϵ_r = 0.5 (broken lines).

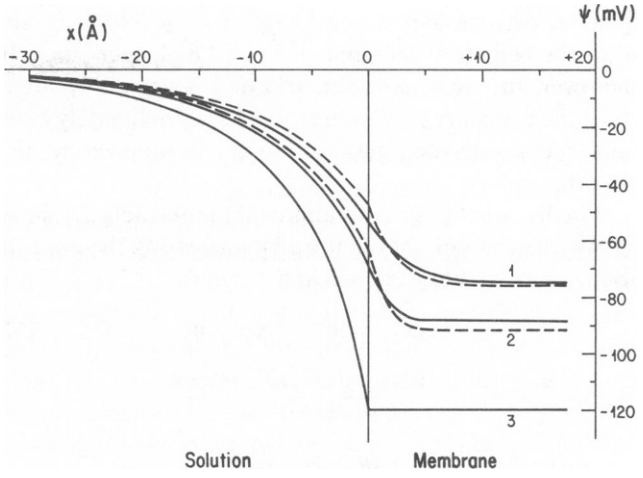

FIGURE 6 The same as in Fig. 5 except for $-eNd = -0.190$ C · m^{-2}.

Figs. 5 and 6 show numerical results for $\psi(x)$ when d = 0, 5, and 10 Å. Here we have varied d, keeping the product Nd constant, i.e., keeping the total amount of membrane fixed charges $-eNd$ per unit area of the surface charge layer ($0 < x < d$) constant ($-eNd$ reduces to the surface charge density σ as $d \to 0$ [Eq. 41]), and using the value $-eNd = -0.0229$ C · m^{-2} in Fig. 5 and -0.190 C · m^{-2} in Fig. 6 so as to give $\psi(d) = -30$ and -120 mV, respectively, as $d \to 0$. The values of the other parameters were chosen to be the same as those used in Figs. 3 and 4. The value of $1/\kappa'$ then becomes 9.6 Å for $\epsilon_r'/\epsilon_r = 1$ and 6.8 Å for $\epsilon_r'/\epsilon_r = 0.5$.

Figs. 5 and 6 indicate a continuous transition from the Donnan potential to the surface potential as d decreases to zero. Figs. 5 and 6 also show a strong dependence of $\psi(x)$ on the thickness d of the surface charge layer; that is, the magnitude of $\psi(x)$ ($0 < x < d$) decreases considerably as d increases. The reason for this lowering of $\psi(x)$ is that the enlarged area inside the membrane into which electrolyte ions are allowed to penetrate increases the shielding effect of the ions upon the membrane fixed charges. We also see from Figs. 5 and 6 that the potential drop within the membrane is sharper for smaller ϵ_r' as in the case of $d = \infty$ (Figs. 3 and 4), which gives rise to less negative values of $\psi(0)$ and more negative values of $\psi(d)$.

DISCUSSION

We have proposed a model for a charged membrane in which the membrane fixed charges are distributed uniformly throughout a surface layer of finite thickness d and we have shown that the potential distribution calculated for our model undergoes a smooth transition from the Donnan potential ($d \to \infty$) to the surface potential ($d \to 0$), showing that the apparent difference between these two concepts is not of a fundamental nature.

Here we have treated symmetrical membranes. When the membrane is unsymmetrical, electrostatic fields can in

general exist inside the core layer ($d < x < h + d$) and thus the boundary condition of Eq. 19 no longer holds. If, however, the right-hand side of Eq. 8 is negligibly small, then the boundary condition of Eq. 19 approximately holds and the results obtained here may be applied to this membrane.

Finally, we will give an approximate formula for small ψ, which can easily be obtained by linearizing the Poisson-Boltzmann equation (Eqs. 3 and 4),

$$\psi(x) = \psi(0)\, e^{-\kappa|x|}, \quad x < 0, \tag{42}$$

$$\psi(x) = \frac{\psi(0)\,[\sinh \kappa'(d - x)] + \psi(d) \sinh \kappa' x}{\sinh \kappa' d} - \frac{kT}{Ze}\frac{N}{2Zn}\left[1 - \frac{\sinh \kappa'(d - x) + \sinh \kappa' x}{\sinh \kappa' d}\right], \quad 0 < x < d, \tag{43}$$

where

$$\psi(0) = -\frac{kT}{Ze}\frac{N}{2Zn}\frac{\sinh \kappa' d}{\sinh \kappa' d + (\epsilon_r/\epsilon_r')^{1/2} \cosh \kappa' d}, \tag{44}$$

$$\psi(d) = -\frac{kT}{Ze}\frac{N}{2Zn}\frac{\sinh \kappa' d + (\epsilon_r/\epsilon_r')^{1/2}(\cosh \kappa' d - 1)}{\sinh \kappa' d + (\epsilon_r/\epsilon_r')^{1/2} \cosh \kappa' d}. \tag{45}$$

We again see that Eqs. 42 and 43 (with Eqs. 44 and 45) give the smooth transition between the Donnan and surface potential. Namely, when $\kappa' d \gg 1$, Eq. 45 reduces to

$$\psi(d) = -\frac{kT}{Ze}\frac{N}{2Zn}, \tag{46}$$

which agrees with the Donnan potential (Eq. 1) for $N/(2Zn) \ll 1$; on the other hand, as $d \to 0$, keeping $\sigma = -eNd$ constant, we obtain from Eq. 44 and 45

$$\psi(0), \psi(d) \to \frac{\sigma}{\epsilon_r \epsilon_0 \kappa}, \tag{47}$$

which is identical to Eq. 2 when $|\sigma/(8n\epsilon_r\epsilon_0\, kT)^{1/2}| \ll 1$.

REFERENCES

Davies, J. T., and E. K. Rideal. 1961. Interfacial Phenomena. Academic Press, Inc., New York and London. 75–84.

Donath, E., and V. Pastushenko. 1979. Electrophoretic study of cell surface properties. The influence of the surface coat on the electric potential distribution and on general electrokinetic properties of animal cells. *Bioelectrochem. Bioenerg.* 6:543–554.

Haydon, D. A. 1961. The surface charge of cells and some other small particales as indicated by electrophoresis. I. The zeta potential-surface charge relationships. *Biochim. Biophys. Acta.* 50:450–457.

Levine, S., M. Levine, K. A. Sharp, and D. E. Brooks. 1983. Theory of the electrokinetic behavior of human erythrocytes. *Biophys. J.* 42:127–135.

Mauro, A. 1962. Space charge regions in fixed charge membranes and the associated property of capacitance. *Biophys. J.* 2:179–198.

Ohki, S. 1965. Rectification by a double membrane. *J. Phys. Soc. Jpn.* 20:1674–1685.

Parsegian, V. A., and D. Gingell. 1973. A physical force model of biological membrane interaction. *In* Recent Advances in Adhesion. L. H. Lee, editor. Gordon & Breach Science Publishers, Inc., New York. 153–192.

Parsegian, V. A. 1974. Possible modulation of reactions on the cell surface by changes in electrostatic potential that accompany cell contact. *Ann. NY Acad. Sci.* 238:362–371.

Teorell, T. 1953. Transport processes and electrical phenomena in ionic membranes. *Prog. Biophys. Biophys. Chem.* 3:305–369.

Verwey, E. J. W., and J. Th. G. Overbeek. 1948. Theory of the stability of lyophobic colloids. Elsevier/North Holland Biomedical Press, Amsterdam. 25–34.

Wunderlich, R. W. 1982. The effects of surface structure on the electrophoretic mobilities of large particles. *J. Colloid Interface Sci.* 88:385–397.